Mapping Psoralen Cross-Links at the Nucleotide Level in Mammalian Cells: Suppression of Cross-Linking at Transcription Factor- or Nucleosome-Binding Sites†

Jun-ichiro Komura,*,‡ Hironobu Ikehata,‡ Yoshio Hosoi,‡ Arthur D. Riggs,§ and Tetsuya Ono‡

Department of Cell Biology, Graduate School of Medicine, Tohoku University, Sendai 980-8575, Japan, and Division of Biology, Beckman Research Institute of the City of Hope, Duarte, California 91010

Received November 3, 2000; Revised Manuscript Received January 30, 2001

ABSTRACT: We have developed a new genomic sequencing method for detecting, with resolution at the nucleotide level, the interstrand DNA cross-links induced by 4,5′,8-trimethylpsoralen along single-copy genes in mammalian cells. The cross-links (diadducts) initially formed are converted into monoadducts by alkali reversal prior to the use of terminal transferase-dependent PCR (TD-PCR). After alkali reversal, but not before, the DNA strands can be separated and used as templates for gene-specific primer extension, which is the first step in the TD-PCR procedure. The converted psoralen adducts block primer extension, and the prematurely terminated single-stranded products are then amplified by TD-PCR and visualized on a sequencing gel. Adducts formed by angelicin, a psoralen derivative that forms only monoadducts, were also investigated by use of TD-PCR. Comparison of the adduct distribution patterns of in vivo-treated DNA with those of in vitro-treated DNA revealed that the binding of transcription factors inhibited both psoralen cross-linking and angelicin monoadduct formation in the c-JUN and c-FOS promoters in living human cells. Adduct formation was also inhibited in the region of a putative positioned nucleosome in the c-FOS promoter. These methods should be of general use for study of in vivo protein−DNA interactions and DNA repair.

A wide variety of DNA-modifying agents have been used as in vivo footprinting agents to probe protein−DNA interactions and chromatin structure in living cells (*1*, *2*). However, only a few methods can provide enough sensitivity to detect the DNA modifications at individual nucleotides within single-copy genes in the highly complex genomes of higher eukaryotes. At present, ligation-mediated polymerase chain reaction (LM-PCR,[1] refs *3*−*5*) is the standard method. LM-PCR is a PCR-enhanced version of the original genomic sequencing method (*6*). LM-PCR recognizes DNA single-strand breaks with 5′-phosphates, and also other DNA modifications that can be converted into strand breaks of this type. Recently, we developed another PCR-enhanced version of genomic sequencing with a wider spectrum of recognizable modifications (*5*, *7*). This method, terminal transferase-dependent PCR (TD-PCR), can detect any modifications that stop DNA polymerase. LM-PCR and TD-PCR have been applied to various DNA-modifying agents including DNA cleaving enzymes and chemicals [e.g., DNase I (*5*), enediyne (*8*)], alkylating agents [dimethyl sulfate (*5*), nitrogen mustard (*9*)], oxidizing agents [$KMnO_4$ (*5*), H_2O_2 (*10*)], bulky chemical carcinogens [benzo[*a*]pyrene (*11*), aflatoxin (*12*)] and ultraviolet light (*5*).

Psoralens are compounds that photoreact covalently and preferentially with double-stranded nucleic acids to form interstrand cross-links and have been used widely as probes to study the structure of DNA and chromatin (reviewed in refs *13*−*16*). Psoralens are especially useful for in vivo studies, because intact living cells are permeable to psoralens, and structures in the cells are not perturbed by the addition of psoralens in the absence of ultraviolet light. The extent of cross-linking upon exposure to ultraviolet light is affected by local chromatin structures such as nucleosome arrays where cross-links form preferentially in the linker DNA between nucleosomes (*17*, *18*). Thus, psoralens seem to be ideal in vivo footprinting agents. However, LM-PCR and TD-PCR are not applicable to DNA cross-linking agents such as psoralens, because interstrand cross-links efficiently inhibit primer annealing (*14*, *19*), which is indispensable to both of the methods. Even under totally denaturing conditions, the cross-links prevent complete separation of the complementary strands of genomic DNA. Under renaturing conditions, the cross-links provide nucleation points for renaturation, and the complementary strands reassociate very rapidly, before the annealing of primers. As a consequence of the unsuitability of these high-resolution detection methods, the regions

† This work was supported by grants from the Ministry of Education, Science, Sports and Culture of Japan (10878080 to T.O. and 12680668 to J.K.), and grants from the United States National Institutes of Health (R01 GM50575 to A.D.R. and P01 CA69449 to Gerald P. Holmquist as P.I.).

* To whom correspondence should be addressed. Phone: +81-22-717-8132. Fax: +81-22-717-8136. E-mail: junkom@mail.cc.tohoku.ac.jp.

‡ Tohoku University.

§ Beckman Research Institute of the City of Hope.

[1] Abbreviations: ANG, angelicin; CRE, cAMP response element; DR, direct repeat; LM-PCR, ligation-mediated PCR; RSRF, related to serum response factor; SIE, sis-inducible element; SRE, serum response element; TCF, ternary complex factor; TD-PCR, terminal transferase-dependent PCR; TMP, 4,5′,8-trimethylpsoralen.

10.1021/bi002539f CCC: $20.00
Published on Web 03/08/2001

with cross-links in extracted genomic DNA have been detected by electron microscopy under denaturing conditions (*17*), or by Southern hybridization after nondenaturing (*20*), denaturing (*16*), or renaturing (*21*) agarose gel electrophoresis. However, these methods of analyzing psoralen cross-links have provided rather low-resolution (0.1−10 kb) information. Recently, development of methods with higher resolution has been attempted (*19*, *22*), but fine mapping of cross-links in the eukaryotic genome has not yet been achieved.

We report here the development of a new method for detecting psoralen cross-links in mammalian cells with resolution at the level of nucleotides. This method is an extended version of TD-PCR. Using this method, we demonstrate that the binding of transcription factors suppresses cross-linking by psoralen as well as monoadduct formation by angelicin in the c-JUN and c-FOS promoters of human fibroblasts. In addition, we show the suppression of adduct formation in the region of a putative translationally positioned nucleosome in the c-FOS promoter.

MATERIALS AND METHODS

Culture and Treatment of Cells. The human diploid fibroblast-like cell line, TIG-3 (*23*), was provided by the Health Science Research Resources Bank (Osaka, Japan). The cells were maintained in Eagle's minimum essential medium supplemented with 10% fetal bovine serum. Three days after inoculation at a density of 1.65×10^6 cells/100 mm dish, the cells were treated with 4,5′,8-trimethylpsoralen (Wako Pure Chemical Industries, Osaka, Japan) or angelicin (Molecular Probes, Eugene, OR) as follows. The medium was removed, and 0.22 mL of a solution of trimethylpsoralen (30 or 100 μM) or angelicin (3 or 10 mM) in ethanol was mixed with 10.8 mL of ice-cold serum-free medium, and poured into the 100 mm tissue culture dish. The cells were incubated on ice for 5 min, and irradiated with 20 kJ/m^2 of long-wavelength ultraviolet light. During irradiation, the plastic lid of the tissue culture dish was replaced with a larger glass lid. The dish was placed on ice and below five FL20S·BLB black-light lamps (Toshiba, Tokyo, Japan). The dose rate under the glass lid was 1.0 kJ/m^2/min, as measured with a UVX radiometer and a UVX-36 sensor (UVP, Upland, CA). The cells were washed twice with cold phosphate-buffered saline and lysed. Isolation of DNA was performed as described (*24*).

Treatment of DNA. DNA isolated from untreated cells was treated in vitro with trimethylpsoralen or angelicin. Eight microliters of a solution of trimethylpsoralen (30 or 100 μM) or angelicin (0.3 or 1 mM) was mixed with 392 μL of a solution of DNA (40 μg) in TE [10 mM Tris (pH 8) and 1 mM EDTA]. After incubation on ice for 2 min, 100 μL droplets of the mixture were placed into a plastic Petri dish with a glass lid on ice, and irradiated with 10 kJ/m^2 of ultraviolet light. NaCl was added to a final concentration of 238 mM before chloroform extraction and 2-propanol precipitation.

Primers and Linkers. We used two sets of primers that were specific for the human c-JUN gene: Primer set JUNA (primer A4, 5′-GAGGGGACCGGGGAACA, nucleotides −280 to −264 relative to the major transcription start site; A2, 5′-GGGGAACAGAGGGCCGAGAGGC, −271 to −250; A3, 5′-GAGAGGCGTGCGGCAGGG, −256 to −239), and primer set JUND (D1, 5′-CCGCGCACCTCCACTC, +52 to +37; D4, 5′-TCCACTCCCGCCTCGCTGCTTC, +43 to +22; D3, 5′-CCTCGCTGCTTCAGCCACACTCA, +33 to +11). Four sets of primers specific for the human c-FOS gene were used: primer set FOSA (A1, 5′-GAACAAGGGTCCGCATTGAA, −479 to −460; A2, 5′-GCATTGAACCAGGTGCGAATGTTCTCTCT, −467 to −439; A3, 5′-TGTTCTCTCTCATTCTGCGCCGTTC, −448 to −424), primer set FOSC (C1, 5′-CGAGGGGCGGAGACAGGT, +126 to +109; C2, 5′-CAGGTGGGCGCTGTGGAGCAGAG, +113 to +91; C3, 5′-AGAGCTGGGTAGGAGCACGGTCACT, +94 to +70), primer set FOSD (D1, 5′-GCGAGCAGTTCCCGTCAATC, −354 to −335; D2, 5′-CCGTCAATCCCTCCCCCCTTACACAG, −343 to −318; D3, 5′-CCCCCCTTACACAGGATGTCCATATTAG, −331 to −304), and primer set FOSE (E1, 5′- TTTATAACAAGCGTTTTATGAATGAGTGTA, −26 to −55; E2, 5′-TGAGTGTAAACGTCACGGGCTCAACCAC, −48 to −75; E3, 5′-GTCACGGGCTCAACCACGGTG, −59 to −79). In each primer set, the first primer was used for primer extension, the second was for PCR, and the third was for probe synthesis. The melting temperature (T_m) of each primer was calculated by the Oligo 4.0 computer program (National Biosciences, Plymouth, MN) with default settings (50 mM salt and 250 pM DNA concentrations). Linkers α and γ, and linker primer have been described (*7*).

Restriction Digestion and Alkali Reversal. One or two micrograms of each sample of trimethylpsoralen or angelicin-treated DNA was digested with 10 units of restriction endonuclease (*Pst*I for c-JUN analysis and *Pvu*II for c-FOS analysis; New England Biolabs, Beverly, MA) in 50 μL of 1 × buffer supplied by the manufacturer, at 37 °C for 2 h. DNA was precipitated by the addition of 50 μL of a salt solution (40 μg of glycogen, 400 mM NaCl, and 15 mM EDTA) and 270 μL of ethanol. The precipitate was dissolved in 10 μL of TE, and 10 μL of 200 mM NaOH was added. The DNA solution was incubated for 30 min at 70 °C unless otherwise indicated, and then neutralized with 10 μL of 200 mM HCl. When the alkali reversal was omitted, the precipitate of restricted DNA was dissolved in 30 μL of TE. In the case of *Stu*I-restricted DNA, only 0.1 μg of DNA per sample was used.

Terminal Transferase-Dependent PCR (TD-PCR). The solution of restricted and alkali-treated DNA was subjected to repeated primer extension, after the addition of 20 μL of extension mix consisting of 2 units of Vent (exo$^-$) DNA polymerase (New England Biolabs), 2.5 × ThermoPol buffer (New England Biolabs), extra 10 mM $MgSO_4$, 625 μM of each dNTP and 50 nM of the first gene-specific primer. For c-FOS analysis, dimethyl sulfoxide (7.5 % v/v) was included in the extension mix (*25*). We employed 10 thermal cycles of 1 min at 95 °C (3 min at 95 °C for the first cycle), 3 min (for c-JUN analysis) or 1 min (for c-FOS analysis) at the T_m of the primer (53−57 °C), and 3 min at 72 °C. After the cycles, the sample was incubated at 95 °C for 1 min. DNA was precipitated by the addition of 50 μL of a salt solution (4 M ammonium acetate and 10 mM EDTA) and 270 μL of ethanol, and the precipitate was dissolved in 10 μL of 0.1 × TE. Following the addition of 10 μL of ribo-tailing mix consisting of 10 units of terminal transferase (GIBCO BRL, Rockville, MD), 2 × buffer supplied by the manufacturer

and 4 mM of rGTP, the sample was incubated at 37 °C for 15 min. DNA was precipitated by the addition of 80 μL of a salt solution (2.5 M ammonium acetate and 3.13 mM EDTA) and 270 μL of ethanol, and then dissolved in 10 μL of TE. Nineteen microliters of ligation mix containing 40 pmol of linker γ in 1.58 × ligase buffer (New England Biolabs), and 1 μL of T4 DNA ligase (400 units/μL, New England Biolabs) were added successively before overnight incubation at 16 °C. For c-JUN analysis, PCR amplification was performed with Vent (exo⁻) DNA polymerase as follows. After the direct addition of 70 μL of amplification mix consisting of 4 units of Vent (exo⁻) DNA polymerase, 1.43 × ThermoPol buffer, extra 2.86 mM $MgSO_4$, 357 μM of each dNTP, 286 nM of the second gene-specific primer and 286 nM of the linker primer, the sample was subjected to 24 thermal cycles of 1 min at 95 °C (3 min at 95 °C for the first cycle), 3 min at 66 °C, and 3 min at 72 °C. The reaction was stopped by the addition of 2 μL of 0.5 M EDTA and 26 μL of 10 M ammonium acetate prior to phenol-chloroform extraction and ethanol precipitation. For c-FOS analysis, PCR was performed with Expand Long Template PCR System (*26*; Roche Diagnostics, Mannheim, Germany), following the precipitation of ligated DNA by the addition of 70 μL of a salt solution (2.86 M ammonium acetate and 7.14 mM EDTA) and 270 μL of ethanol. The PCR mixture (50 μL) containing 2.63 units of polymerases, 1 × buffer 3, extra 0.75 mM $MgCl_2$, 500 μM of each dNTP and 300 nM of each primer was subjected to 24 thermal cycles of 1 min at 95 °C (3 min at 95 °C for the first cycle), 1 min at 63 °C, and 3 min at 68 °C. The 68 °C step was extended by 20 s/cycle from the 11th cycle. The reaction was stopped by the addition of 50 μL of a salt solution consisting of 4 M ammonium acetate and 10 mM EDTA before phenol-chloroform extraction and ethanol precipitation.

Electrophoresis of the PCR products through a denaturing 8% polyacrylamide gel, transfer to a charged nylon membrane by electroblotting, and hybridization with a radiolabeled single-stranded probe were performed as described (*5*). We synthesized the probe by repeated primer extension on a double-stranded template, which was a DNA fragment prepared by PCR. Fragments from nucleotide position −418 to −69 and from −256 to +214 were used for primer sets JUNA and JUND, respectively. In all c-FOS experiments, a fragment from −448 to +94 was used. The labeling mixture (60 μL) contained 10 ng of the DNA fragment, 500 nM of the third gene-specific primer, 5 units of Taq DNA polymerase (Takara Shuzo, Otsu, Japan), 1 × buffer supplied by the manufacturer, 0.56 μM of [α-^{32}P]dCTP (110 TBq/mmol), and 16.7 μM of each of dATP, dGTP, and dTTP. We employed 30 thermal cycles of 0.5 min at 95 °C (2 min at 95 °C for the first cycle), 1 min at (T_m − 3) °C and 1 min at 72 °C. After hybridization and washes, the nylon membrane was exposed to BioMax MR film (Eastman Kodak, Rochester, NY) without intensifying screens, and the autoradiograph visually inspected. Differences in band intensity were confirmed by quantification with a BAS-1500 imaging plate scanner (Fuji Photo Film, Tokyo, Japan).

Ligation-Mediated PCR (LM-PCR). By modifying the TD-PCR procedure described above, we carried out LM-PCR at the same time. Without restriction or alkali reversal, 0.6 μg of chemically cleaved (*27*) genomic DNA was subjected to only one cycle of primer extension. Incubation at 95 °C after the cycle was omitted. Ribo-tailing was also omitted. Linker α was used in place of linker γ. The use of Vent (exo⁻) DNA polymerase in the PCR step of LM-PCR sometimes gave poor sequence ladders; the use of Expand Long Template PCR System produced better results.

RESULTS

The psoralen molecule has a planar tricyclic structure with two photoreactive sites, the 3,4-pyrone and the 4′,5′-furan double bonds (Figure 1A). Initially, it interacts with double-stranded DNA noncovalently by intercalation (Figure 1B). Upon absorption of a photon of long-wavelength ultraviolet light, one of its photoreactive sites reacts with the 5,6 double bond of a pyrimidine residue, principally a thymine, forming a covalent cyclobutyl bond that links the psoralen molecule to one strand of DNA. Photoreaction at the 3,4-pyrone double bond of psoralen yields a pyrone-side monoadduct; reaction at the 4′,5′-furan double bond yields a furan-side monoadduct. The furan-side monoadduct can form a diadduct (interstrand cross-link) on absorption of a second photon, if a pyrimidine is available for reaction at the adjacent position on the opposite strand of DNA. The pyrone-side monoadduct cannot form a diadduct because it does not absorb long-wavelength ultraviolet light.

TD-PCR is essentially a polymerase stop assay (Figure 1C). Any DNA lesion or modification that stops extension from a gene-specific primer with DNA polymerase can be detected. The prematurely terminated single-stranded products of the primer extension are visualized on a sequencing gel, after a two-step amplification consisting of linear amplification by repeated primer extension and then exponential amplification by PCR. TD-PCR has not been applicable to psoralen cross-links because cross-linked genomic DNA renatures rapidly and prevents primer annealing. To circumvent this problem, we converted the cross-links into monoadducts before subjecting the DNA to TD-PCR. We carried out this conversion utilizing alkali reversal of furan-side cyclobutyl bonds. Shi et al. (*28*) and Yeung et al. (*29*) have reported that incubation under alkaline conditions at elevated temperatures reverses furan-side cyclobutyl bonds, and that pyrone-side cyclobutyl bonds are resistant to this treatment. By alkali reversal, cross-links are converted into pyrone-side monoadducts, and furan-side monoadducts are eliminated, whereas pyrone-side monoadducts persist (Figure 1B). 4-Methylated psoralens including 4,5′,8-trimethylpsoralen, which we used in the present study, have an overwhelming preference (∼98%) for addition at the furan side; only ∼2% of the total adducts are pyrone-side monoadducts (*30*, *31*). Therefore, the trimethylpsoralen adducts detected by TD-PCR after completion of alkali reversal should be exclusively pyrone-side monoadducts, the vast majority of which should originally have been cross-links.

Figure 2 shows the results of a representative experiment to determine the appropriate conditions of alkali reversal. Genomic DNA was extracted from human diploid fibroblasts, treated in vitro with trimethylpsoralen plus ultraviolet light, restricted with *Pst*I, and then, before the primer extension step of TD-PCR, incubated in 100 mM NaOH for 30 min at different temperatures. Adducts on the lower strand of the c-JUN promoter region were analyzed. After alkali reversal,

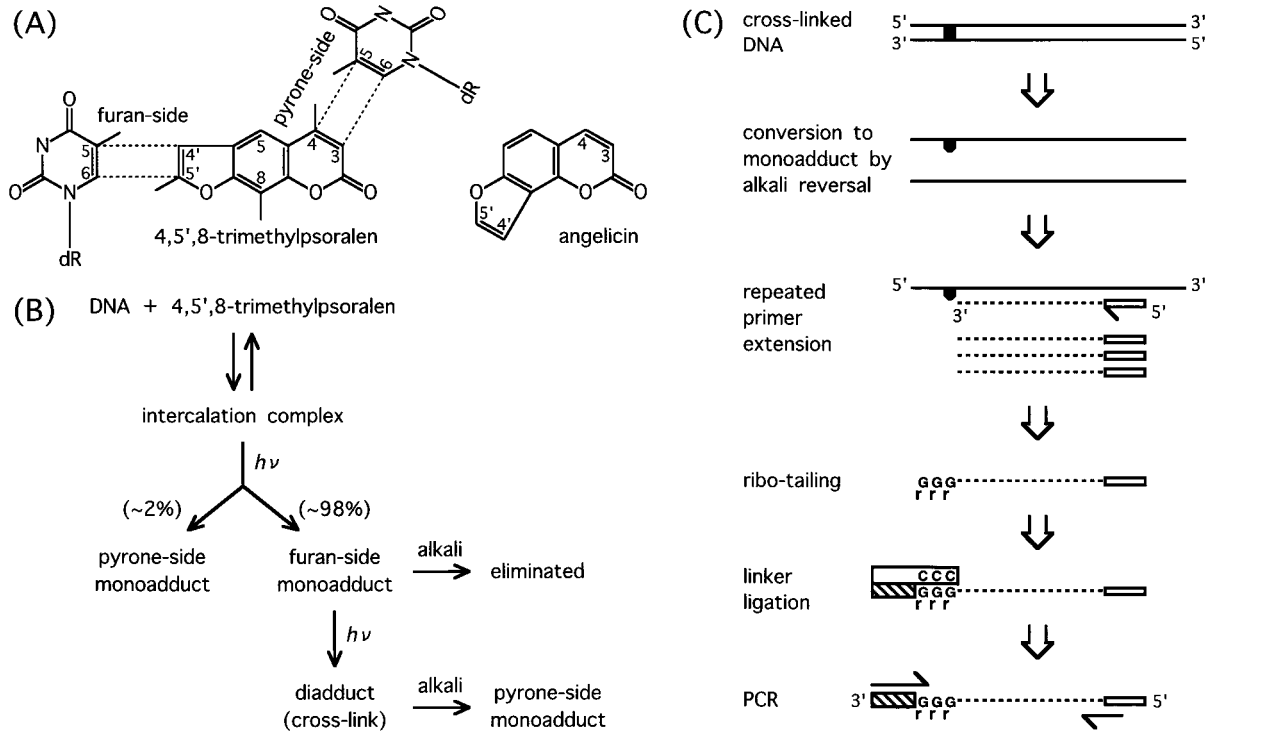

FIGURE 1: (A) Structure of 4,5′,8-trimethylpsoralen and angelicin. Two possible cyclobutyl bonds between the trimethylpsoralen molecule and thymine bases are drawn with dotted lines. (B) Interaction of trimethylpsoralen with DNA to form three types of adducts, and conversion of the adducts by alkali reversal of furan-side cyclobutyl bonds. (C) Outline of cross-link detection by alkali reversal and TD-PCR.

strong bands were seen at specific nucleotide positions (lanes 17 and 18). When alkali reversal was omitted, no bands were observed (lane 15). These results suggest that almost every genomic DNA molecule of the 1.6 kb *Pst*I restriction fragment containing the c-JUN promoter region (*32*) had at least one cross-link. When alkali reversal was performed at 55 °C, faint bands appeared (lane 16), whereas incubation at 70 °C gave rise to much stronger signals (lane 17). Most of the signals were seen at the sites of 5′-TA and 5′-AT sequences. The sequence preference of trimethylpsoralen cross-linking has been reported to follow the pattern 5′-TA > 5′-AT ≫ 5′-TG > 5′-GT (*33*). Under our experimental conditions, strong signals were detected at all of the 5′-TA sites in the case of DNA treated in vitro. However, bands were not observed at some of the 5′-AT sites and at many of the 5′-TG sites. At all of the 5′-GT sites, bands were undetectable. Alkali reversal at a higher temperature (85 °C) did not increase the intensity of the bands at the 5′-TA and 5′-AT sites (lane 18). Instead, numerous new minor bands appeared at various positions throughout the lane. We concluded that practically all cross-links were converted into monoadducts by incubation at 70 °C and used this temperature in footprinting experiments thereafter. We assume that the minor bands seen in the sample incubated at 85 °C resulted from the induction of lesions on the genomic DNA template by hot alkali, although there is a possibility that hot alkali revealed preexistent alkali-sensitive lesions. As the sequence specificity of the minor bands is not apparent, the nature of the lesions is unknown.

Genomic DNA treated in vitro with angelicin plus ultraviolet light was also subjected to alkali reversal and TD-PCR analysis. Angelicin (Figure 1A) is a monofunctional psoralen derivative. Although it has two photoreactive sites, it cannot form interstrand cross-links because of its angular geometry (*13*, *34*). We used this psoralen derivative to examine whether our system was adequate for detection of psoralen monoadducts. Intense bands were seen when alkali reversal was not done (Figure 2, lane 11). This result is consistent with the expectation that angelicin forms only monoadducts. Comparison of the band pattern of lane 11 with that of lane 17 confirms the similarity between the sequence preference of monoadduct formation by angelicin (*35*) and that of cross-linking by trimethylpsoralen (*33*). Alkali reversal of angelicin-treated DNA at 70 °C decreased the band intensity, but only to a limited extent (lane 13), suggesting that angelicin, a psoralen derivative without the 4-methyl group, probably formed a considerable number of alkali-resistant pyrone-side monoadducts. Incubation of angelicin-treated DNA at 85 °C produced a substantial number of new minor bands (lane 14), with a pattern similar to that seen for trimethylpsoralen at 85 °C (lane 18).

We noticed that the signals from some of the neighboring 5′-TA or 5′-AT sequences could not be separately distinguished. For example, in the 5′-ATA sequence at nucleotides −56 to −58 (indicated by the fifth diamond from the top), distinguishing the signal of the 5′-AT from that of the 5′-TA is theoretically impossible, because adducts are formed on the single T residue. The sequence 5′-ATGAT at nucleotides −63 to −67 (indicated by two neighboring circles) is ∼200 bp away from the primers used, and the resolution at this distance on the sequencing gel is not very high. In addition, the heterogeneity in the position of the termination of primer extension, the heterogeneity in the number of incorporated ribonucleotides, and the presence of single-base 3′ overhangs in some of the PCR products may cumulatively produce two to four bands at one adduct position (*7*, *24*). As a result, it was difficult to separate the signals of two 5′-AT sequences.

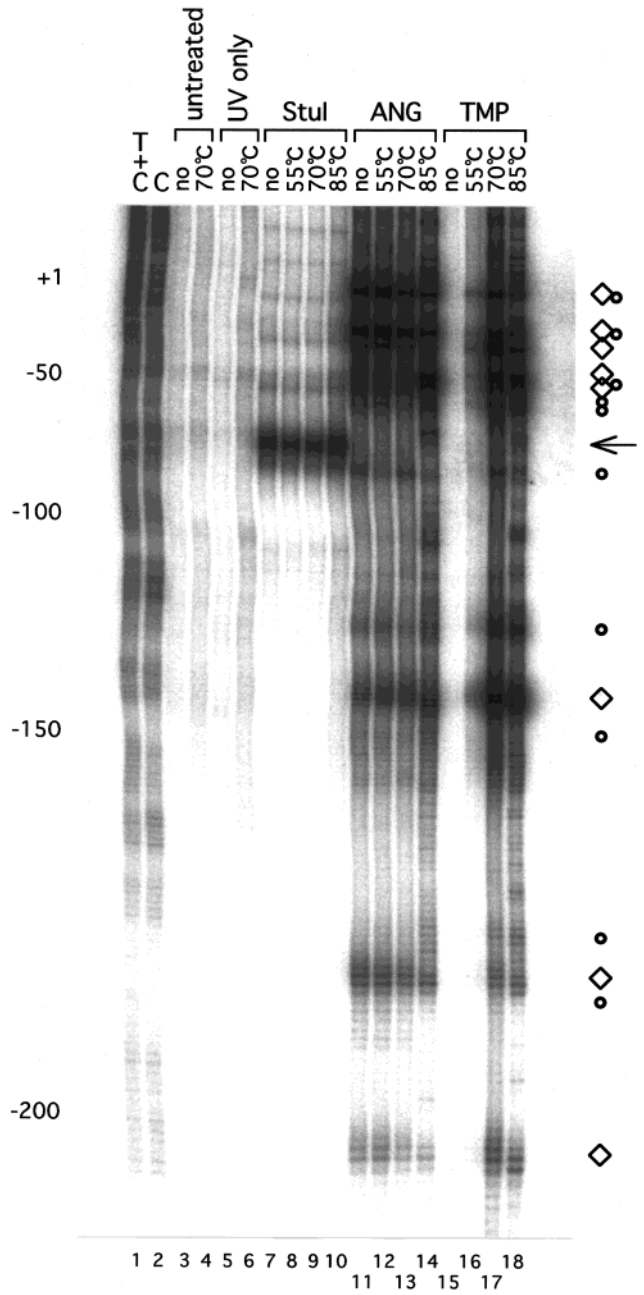

FIGURE 2: Effect of alkali reversal on detection by TD-PCR of psoralen adducts on the lower strand of the human c-JUN promoter region. DNA from human diploid fibroblasts was treated in vitro with 20 μM angelicin (ANG) and 10 kJ/m^2 ultraviolet (UV) light (lanes 11−14); 2 μM trimethylpsoralen (TMP) and UV (lanes 15−18); UV only (lanes 5 and 6); restricted with *Stu*I (lanes 7−10); or untreated (lanes 3 and 4). Alkali reversal was either performed at the indicated temperature, or not performed (lanes labeled "no"), before TD-PCR with primer set JUNA. DNA cleaved by the method of Maxam and Gilbert (T+C, C) was subjected to LM-PCR instead of TD-PCR. The products of TD-PCR are usually two to three nucleotides longer than those of LM-PCR (*7*). The numbers on the left indicate the nucleotide positions of the LM-PCR signals relative to the major transcription start site. Diamonds and circles on the right indicate the locations of 5′-TA and 5′-AT sequences, respectively. The arrow indicates the *Stu*I restriction site.

The possible influence of alkali treatment on detection of another type of DNA modification (strand breaks) also was examined (lanes 7−10). Alkali treatment of *Stu*I-restricted genomic DNA did not change the band pattern. This result shows that alkali treatment does not interfere with the detection of strand breaks. However, we would like to point out that some kinds of DNA modifications are converted into strand breaks under alkaline conditions, and can be detected as "alkali-labile sites" (*36*). Since long-wavelength ultraviolet light, which is used for psoralen cross-linking, may potentially induce various lesions including alkali-labile ones (*37*), it should be verified by appropriate controls that the bands observed in the psoralen lanes result from psoralen adducts, not from other lesions. Unlike trimethylpsoralen- or angelicin-treated DNA, *Stu*I-restricted DNA did not generate newly detectable minor bands when incubated at 85 °C (lane 10). However, it should be noted that only 0.1 μg of *Stu*I-restricted DNA/sample was used instead of 1 μg of trimethylpsoralen- or angelicin-treated DNA. The influence of ultraviolet irradiation and alkali treatment on background signals was also examined (lanes 3−6). Ultraviolet irradiation of genomic DNA in the absence of psoralens did not increase the background (lane 5). Alkali treatment of unirradiated (lane 4) or irradiated (lane 6) DNA at 70 °C increased the background only slightly.

We next investigated the distribution of the cross-links induced by trimethylpsoralen in vivo, as well as that of the monoadducts induced by angelicin in vivo. Both strands of the same region as in Figure 2 were analyzed with two sets of primers. The human c-JUN promoter was chosen because this compact promoter (∼200 bp) contains several transcription factor binding sites whose constitutive occupancy, irrespective of the transcription status, has been demonstrated by in vivo footprinting with DNase I, dimethyl sulfate or ultraviolet light (*38*−*40*; see Figure 4). Living cells were treated with a psoralen plus ultraviolet light, and then the genomic DNA was extracted and analyzed. The resultant patterns of in vivo adduct formation were compared with those of in vitro formation. Figure 3 shows the adduct distributions on the lower strand of the c-JUN promoter. We selected adduct-forming conditions that gave similar levels of signal intensity both in vivo and in vitro. While comparable conditions were used for both in vivo and in vitro trimethylpsoralen cross-linking treatments (0.6 or 2 μM trimethylpsoralen and 20 J/m^2 ultraviolet light for in vivo versus the same concentrations and 10 J/m^2 for in vitro), much stronger conditions were used for in vivo angelicin monoadduct formation than for in vitro formation (60 or 200 μM angelicin and 20 J/m^2 ultraviolet light for in vivo versus 6 or 20 μM and 10 J/m^2 for in vitro). This difference between trimethylpsoralen and angelicin might reflect increased hydrophobicity and increased affinity to DNA of methylated psoralens (*13*, *34*).

The in vivo formation patterns of both trimethylpsoralen cross-links and angelicin monoadducts were generally similar to their in vitro counterparts. The adducts were formed predominantly at 5′-TA and 5′-AT sequences both in vitro and in vivo. However, there were some remarkable differences. For example, the 5′-TA sequence at nucleotides −188 and −189 (indicated by an arrow in Figure 3) was a preferred site for in vitro formation of both angelicin monoadducts (lanes 3 and 4) and trimethylpsoralen cross-links (lanes 7 and 8), but formation of these adducts in vivo was negligible (lanes 5, 6, 9, and 10). This 5′-TA sequence is within a binding site of the transcription factor AP-1. The 5′-AT sequence at nucleotides −130 and −131 (indicated by another arrow) was protected from trimethylpsoralen cross-

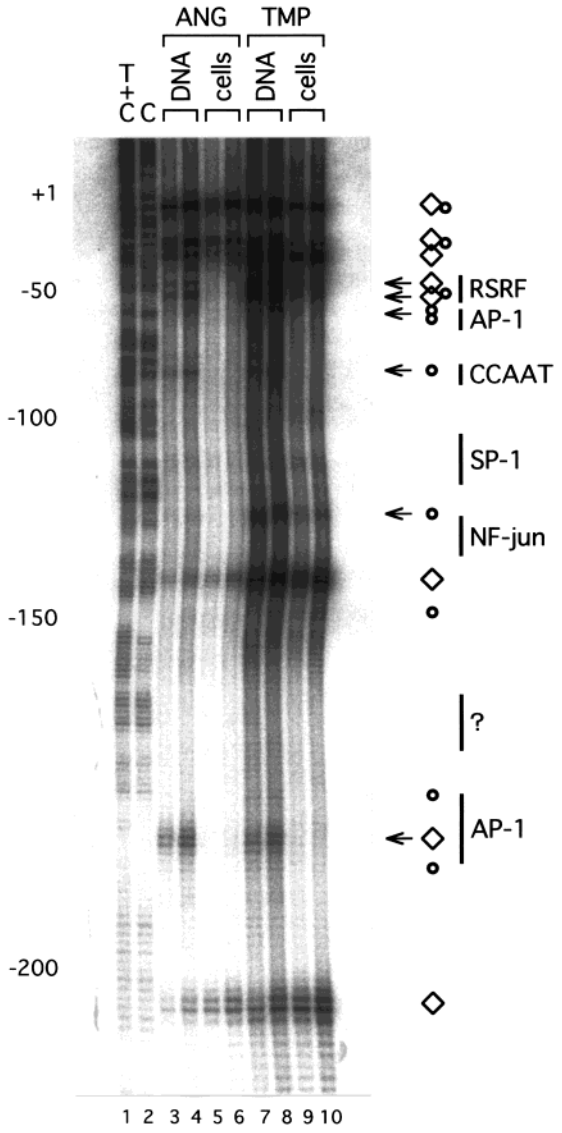

FIGURE 3: In vitro and in vivo formation of psoralen adducts on the lower strand of the c-JUN promoter. Primer set JUNA was used. The monoadducts induced by angelicin (ANG) were analyzed by TD-PCR, and the cross-links induced by trimethylpsoralen (TMP) were analyzed by alkali reversal plus TD-PCR. Lanes labeled "DNA" denote the samples of DNA treated in vitro, and lanes labeled "cells" denote the samples of DNA from the cells treated in vivo. The final concentration of angelicin or trimethylpsoralen was 6 μM (lane 3), 20 μM (lane 4), 60 μM (lane 5), 200 μM (lane 6), 0.6 μM (lanes 7 and 9), or 2 μM (lanes 8 and 10). The dose of ultraviolet light was 10 kJ/m^2 (lanes 3, 4, 7, and 8) or 20 kJ/m^2 (lanes 5, 6, 9, and 10). The numbers on the left indicate the nucleotide positions relative to the major transcription start site. Diamonds and circles on the right indicate the locations of 5′-TA and 5′-AT sequences, respectively. Arrows indicate the sites of decreased adduct formation in vivo. Vertical bars indicate the binding sites of known transcription factors and an unknown factor revealed by in vivo footprinting with DNase I, dimethyl sulfate or ultraviolet light.

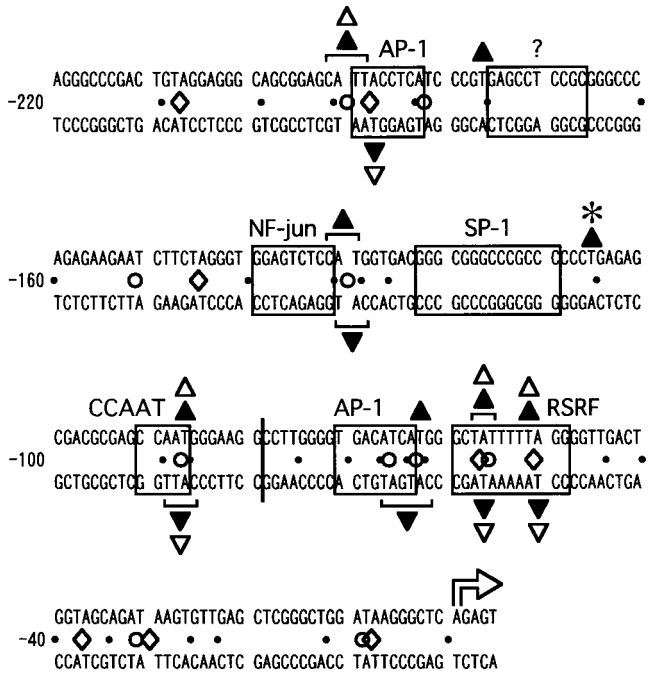

FIGURE 4: Summary of the distribution of the sites of decreased formation of psoralen adducts in vivo on both strands of the human c-JUN promoter. The arrow indicates the major transcription start site. The numbers on the left indicate the nucleotide positions relative to the transcription start site. The vertical line represents the *Stu*I restriction site. Boxes represent the consensus recognition sequences of transcription factors whose binding has been shown by in vivo footprinting with DNase I, dimethyl sulfate or ultraviolet light. Diamonds, circles and dots represent the locations of 5′-TA, 5′-AT, and 5′-TG sequences, respectively. Open triangles represent the sites of decreased formation of angelicin-induced monoadducts in vivo. Solid triangles represent the sites of decreased formation of trimethylpsoralen-induced cross-links in vivo. However, the triangle with an asterisk indicates the site of enhanced adduct formation, not decreased formation. The cross-links with different orientations were analyzed separately; only the cross-links whose pyrone sides were attached to the analyzed strand were detected. Brackets indicate that the signals of the neighboring pyrimidines were inseparable.

linking in vivo, but the protection was only partial. This sequence is at the periphery of the binding site of NF-jun. Four other sites of decreased formation of adducts in vivo are also indicated by arrows in Figure 3. They are within the binding site of the transcription factor RSRF (related to serum response factor), within another AP-1 binding site, or within a CCAAT box. All of the protected sites are in or near the sequences that have been shown to bind transcription factors in vivo. Therefore, we conclude that the suppression of adduct formation in vivo can be attributed to protein binding and that these sites are the footprints of transcription factors. At the 5′-ATGAT sequence at nucleotides −63 to −67 (in one of the binding sites of AP-1) and at the 5′-AT sequence at nucleotides −130 and −131 (near the binding site of NF-jun), we could discern footprints only in the trimethylpsoralen lanes. The signals of angelicin monoadducts at these sequences were very weak, and we could not recognize them as bands.

Figure 4 summarizes the results of our in vivo footprinting experiments on both strands of the c-JUN promoter. On the upper strand, we were able to see footprints at all of the sites opposite the footprint sites on the lower strand. In addition, we found protection from trimethylpsoralen cross-linking at the 5′-TG sequence at nucleotides −177 and −176 [on the periphery of the binding site of an unknown factor (*39*)] on the upper strand. This footprint is exceptional because 5′-TG sequences are not preferred targets for adduct formation and are not usually available for footprinting analysis. It should be noted that the trimethylpsoralen cross-links detected by the analysis of the upper strand and those detected by the analysis of the lower strand belong to

different subgroups, even at the same 5′-TA or 5′-AT site. The analysis of one strand detects only the cross-links with the alkali-resistant pyrone-side cyclobutyl bonds on the analyzed strand. Analyzing the cross-links with different orientations separately, however, revealed similar footprint patterns. We could not detect any protection within the SP-1 binding site at nucleotides −123 to −110; this site is composed of only G and C residues and does not contain any target sequences for psoralen. However, we found weak enhancement of trimethylpsoralen cross-linking at the 5′-TG sequence at nucleotides −106 and −105, just outside the SP-1 binding site on the upper strand. This is the only hyper-reactive site detected in the c-JUN promoter.

Finally, we performed footprinting of both strands of the promoter region (∼350 bp) of the human c-FOS gene. In the c-FOS promoter, there are two domains important for transcriptional regulation (*41*, *42*): one is just upstream of the transcription start site; the other is around position −300. In these domains, several transcription factor binding sites that are constitutively occupied in living cells have been identified by footprinting studies with dimethyl sulfate or ultraviolet light (*40*, *43*−*46*; see Figure 7). Figure 5 shows our in vivo psoralen footprinting analysis of the upper strand. We used a different polymerase system [Taq plus Pwo instead of Vent (exo⁻)] in the PCR step of TD-PCR when analyzing the c-FOS promoter. It improved the signal intensity especially at some of the less preferred 5′-TG sequences, making more sites available for footprinting. A very strong footprint was seen in the 5′-ATATTA sequence at nucleotides −310 to −305, where adduct formation was completely suppressed in vivo. This sequence is within the serum response element (SRE). In contrast, we found incomplete protection at the 5′-TA sequence at nucleotides −55 and −54. These nucleotides are at the periphery of the cAMP response element (CRE). In the trimethylpsoralen lanes, weak signals at the 5′-TG sequence at nucleotides −85 and −84 inside the direct repeat (DR) were suppressed. There was also a 5′-TG sequence at nucleotides −70 and −69 between the CRE and the DR with hyporeactivity for trimethylpsoralen cross-linking as well as for angelicin monoadduct formation.

We found prominent protection in the sequence 5′-ATTA at nucleotides −180 to −177. Minor bands around this site in the trimethylpsoralen lanes were also suppressed. Scrutiny of this region with a more upstream primer set (data not shown) and analysis of the opposite strand (Figure 6) revealed many sites of protection from adduct formation. The protected sites (and also a hyper-reactive site) were distributed in the area from position −220 to −137, and most were 5′-TG sequences. The results of our footprinting experiments on both strands of the c-FOS promoter with four sets of primers are summarized in Figure 7. The protection area upstream of the DR seems too extensive to be the footprint of a single transcription factor. So far, in vivo footprints of any transcription factors have not been reported in this large protection area. At nucleotides −179 to −164, Runkel et al. (*44*) found a sequence that resembles the consensus binding sequence for NF-1, but their dimethyl sulfate footprinting analysis failed to detect any occupancy over this sequence in living cells. Interestingly, both in vivo (*42*) and in vitro (*47*) studies have shown the presence of a positioned nucleosome in the c-FOS promoter. By using micrococcal

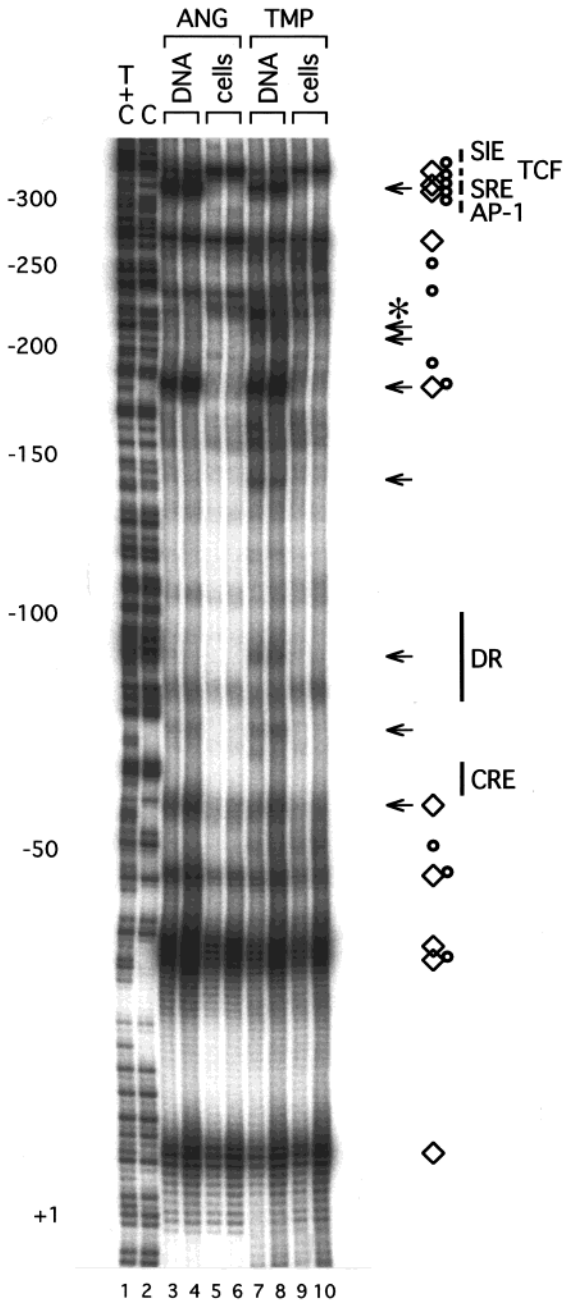

FIGURE 5: In vitro and in vivo formation of psoralen adducts on the upper strand of the c-FOS promoter. Primer set FOSC was used. Lanes and symbols are identical to those in Figure 3, except that the asterisk indicates the site of enhanced formation of angelicin monoadducts. Arrows without diamonds or circles indicate protection at 5′-TG sequences.

nuclease digestion and Southern hybridization, Herrera et al. (*42*) identified a positioned nucleosome principally in the region from −250 to −90 in living cells (indicated by horizontal lines in Figure 7). The large area of protection from psoralens in our study is in the middle of the region bound by this nucleosome. Therefore, we assume that this protection area is the footprint of the putative positioned nucleosome, although there remains the possibility that it is the footprint of a complex of NF-1 and/or other factors. Electron microscopy of DNA under denaturing conditions has revealed that a region of ∼160 bp is protected by a nucleosome from extensive psoralen cross-linking (*17*, *48*), but our footprint (84 bp) is shorter than this length. In

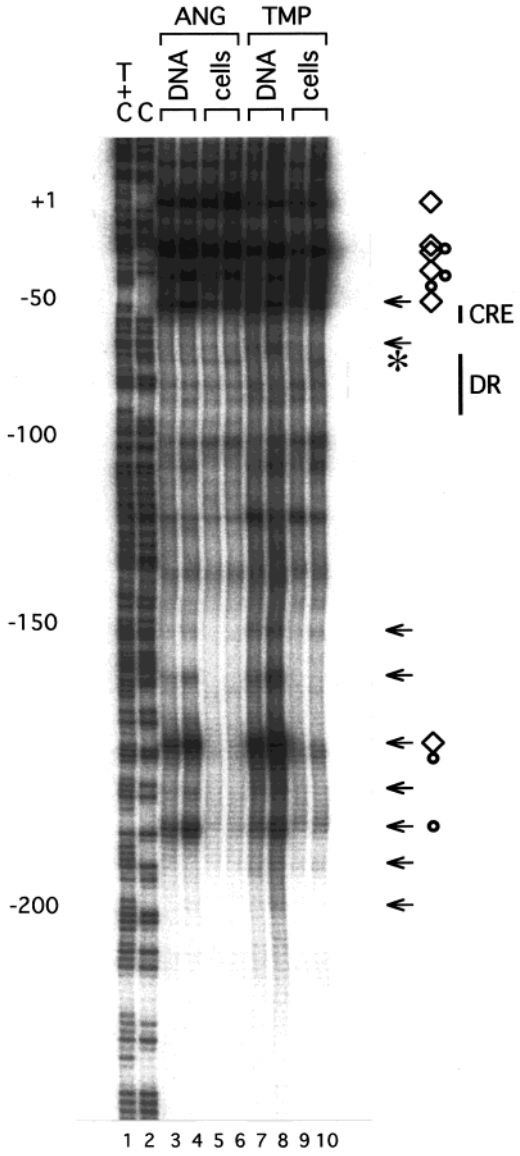

FIGURE 6: In vitro and in vivo formation of psoralen adducts on the lower strand of the c-FOS promoter. Primer set FOSD was used. Lanes and symbols are identical to those in Figure 3, except that the asterisk indicates the site of enhanced formation of trimethylpsoralen cross-links.

addition to the principal position of the nucleosome in the c-FOS promoter, multiple overlapping positions have been suggested to occur both in vivo and in vitro (*42*, *47*). It is probable that only the overlapping region is well protected from psoralens, and this is the region that corresponds to our footprint. Alternatively, the paucity of preferred 5′-TA sequences in this G+C-rich region (only one 5′-TA in the 161 bp region of the putative positioned nucleosome) and the dependence of footprint discernment on weak signals at 5′-TG sequences might lead to underestimation of the length of the footprint.

In addition to many sites of protection from adduct formation, we found two sites of enhanced formation in the c-FOS promoter. One is a modestly hyper-reactive site for the formation of angelicin monoadducts at nucleotides −220 and −219 at the edge of the large protection area on the upper strand. The other is a weakly hyper-reactive site for trimethylpsoralen cross-linking at nucleotides −78 and −79 on the periphery of the DR on the lower strand.

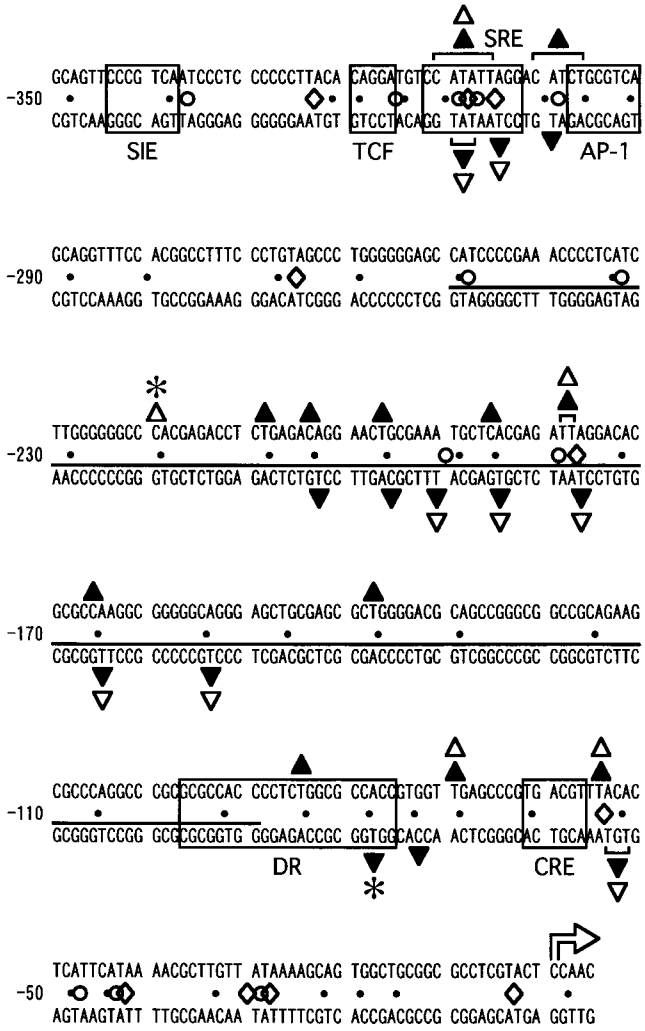

FIGURE 7: Summary of the distribution of the sites of decreased formation of psoralen adducts in vivo on both strands of the human c-FOS promoter. Horizontal lines represent the region occupied by a putative positioned nucleosome (*42*). Other symbols are identical to those in Figure 4.

DISCUSSION

Psoralens have been used for both in vitro (*49*) and in vivo (*50*) footprinting studies, and the excellence of psoralens in detection of protein−DNA interactions has been well established. However, in vivo footprinting experiments with psoralens have usually been performed with low resolution in small genomes, e.g., mitochondrial DNA (*50*), because of the lack of appropriate methods. Recently, by use of trimethylpsoralen and a procedure consisting of λ exonuclease digestion and primer extension, Wellinger and Sogo (*22*) were able to map nucleosomes on a yeast minichromosome with a resolution of about 30 bp. By primer extension followed by PCR, Oh and Hanawalt (*19*) were able to determine the distribution of adducts with resolution at the nucleotide level in mammalian genomic DNA treated with a psoralen in vitro, when monoadducts were formed selectively by irradiation with ∼410 nm light. When cross-linking conditions (∼360 nm ultraviolet) were used, however, their method was unable to detect adduct formation, confirming the inhibitory effect of cross-links on primer annealing. In the present study, we have determined the distribution of psoralen cross-links at the level of nucleotides in single-copy

genes in mammalian cells for the first time. The successful detection of the in vivo footprints confirms the useful capacity of psoralens as footprinting agents.

Most of the footprints detected in this study resulted from the protection of sites from psoralen adduct formation in vivo, but three sites of enhanced formation were also observed. Footprints are very conspicuous when 5′-TA sequences are inside the transcription factor binding sites; intense signals at the preferred targets in the in vitro lanes are suppressed almost completely in the in vivo lanes. At 5′-AT and 5′-TG sequences, discernment of footprints is more difficult because of the weaker signals. When the target sequences are at the boundaries of the binding sites, the signals may be suppressed partially, or enhanced weakly. Most of the footprints are detected on both upper and lower strands and both by angelicin footprinting and by trimethylpsoralen footprinting, especially at the 5′-TA sequences. At some of the less preferred 5′-AT and 5′-TG sequences, however, footprints can be discerned only on one strand, or only for one kind of psoralen. This does not necessarily mean that the footprints are not generated on the other strand or by the other psoralen, but probably is simply because the quantity of the adduct is not high enough for signal detection and footprint discernment at these sites.

The mechanisms responsible for the formation of psoralen footprints are not fully known. Psoralen cross-linking consists of three steps (Figure 1B): (i) intercalation, (ii) the first photoreaction to form a monoadduct, and (iii) the second photoreaction to form a cross-link. Probably the last step does not contribute to the formation of footprints, because angelicin, a monofunctional psoralen, also generates footprints. It has been argued that the intercalation into the DNA double helix determines the stereospecificity and distribution of psoralen adducts (*13*). Assuming this is correct, the constraint imposed by the distortion of the DNA helices that bind proteins may prevent psoralen molecules from intercalating. As to the hyper-reactive sites, we suppose that psoralen intercalation may be promoted by the slight unwinding of DNA at some of the boundaries of protein binding sites, for it has been demonstrated that trimethylpsoralen reacts with negatively supercoiled DNA faster than with relaxed DNA (*51*, *52*).

The footprint patterns obtained by the analysis of angelicin monoadducts are generally similar to those obtained by the analysis of trimethylpsoralen cross-links. The capacity of monofunctional psoralens to reveal protein−DNA interactions and chromatin structure has not yet been thoroughly investigated, in marked contrast to that of cross-linking psoralens. If the capacity of angelicin is similar to that of cross-linking psoralens, angelicin may be a very promising footprinting agent.

Because of their strong sequence specificity, psoralens have limited numbers of targets in DNA, like other cell-permeable footprinting agents (*1*, *2*) such as dimethyl sulfate, which alkylates G residues, and ultraviolet light, which dimerizes neighboring pyrimidines. We have previously used both dimethyl sulfate and ultraviolet light to scan the promoter region of the mouse Xist gene for transcription factor binding sites, because they complement each other with respect to the target sequences (*24*). In the case of psoralens, this kind of complementation may also be necessary for covering all parts of a DNA region.

In addition to the usefulness of psoralens in the detection of in vivo binding of transcription factors to DNA, which was shown in this study, psoralens have great potential as nucleosome footprinting agents (*1*, *2*), because they can effectively detect DNA regions occupied by nucleosomes in vivo (*17*, *18*). Psoralens are considered superior to nucleases, which are currently used for detection of positioned nucleosomes, in that psoralens do not require permeabilized cells or isolated nuclei, and they do not disrupt the structures of protein−DNA complexes by cleaving DNA. Assuming that the large area of protection in the middle of the c-FOS promoter in our study is the footprint of a positioned nucleosome, it will be interesting to investigate changes in the footprint when the transcription of the gene is activated or repressed, as it has been suggested that conformational changes of histone H3 (*53*) and chromatin remodeling by the SWI/SNF complex (*54*) are involved in the transcriptional control of the c-FOS gene. However, we would like to point out it is not certain that the large area of protection from psoralens is due to a true nucleosome. Our psoralen analysis is somewhat limited by the fact that there is only one 5′-TA sequence in the 161 bp region of the putative positioned nucleosome, and the previous data suggesting the nucleosome was not conclusive. Nevertheless, it seems clear that combining psoralen treatment with TD-PCR adds a new and powerful assay for detection of chromatin fine structure and changes in this structure.

Our method of detecting cross-links virtually excludes detection of monoadducts formed by trimethylpsoralen, because the formation of pyrone-side monoadducts by this agent is negligible, and alkali reversal eliminates furan-side monoadducts. We believe the repair of cross-links also can be better studied by use of the techniques reported here, although caution is needed against contaminating monoadducts. It is very important to strictly distinguish cross-links from monoadducts in repair analysis, because cross-links require special repair pathways that involve recombination (*37*). In addition to alkali reversal, there are at least two other procedures that in theory can be combined with LM-PCR or TD-PCR for the purpose of detecting cross-links. One is the utilization of λ exonuclease, which can expose the template strand of cross-linked DNA by digesting the complementary strand in the 5′ to 3′ direction until it reaches the sites of adducts (*22*). Primer extension following this, however, will not discriminate between cross-links and monoadducts. The other possible procedure is the utilization of *Escherichia coli* UvrABC endonuclease, which recognizes a wide spectrum of bulky adducts. UvrABC has been used successfully with LM-PCR (*11*), and should also be useful for the detection of psoralen adducts. However, quantitative studies of cross-link repair might be impossible because of the characteristics of UvrABC endonuclease. This enzyme recognizes furan-side and pyrone-side monoadducts as well as cross-links (*55*). Even under optimal conditions, it incises the DNA with low efficiency, and only a fraction of the adducts are converted into strand breaks (*56*). We believe the employment of alkali reversal is superior, especially when a 4-methylated psoralen is used.

REFERENCES

1. Zaret, K. S. (1999) *Methods Enzymol. 304*, 612−626.
2. Simpson, R. T. (1999) *Curr. Opin. Genet. Dev. 9*, 225−229.

3. Mueller, P. R., and Wold, B. (1989) *Science 246*, 780−786.
4. Pfeifer, G. P., Steigerwald, S. D., Mueller, P. R., Wold, B., and Riggs, A. D. (1989) *Science 246*, 810−813.
5. Pfeifer, G. P., Chen, H. H., Komura, J., and Riggs, A. D. (1999) *Methods Enzymol. 304*, 548−571.
6. Church, G. M., and Gilbert, W. (1984) *Proc. Natl. Acad. Sci. U.S.A. 81*, 1991−1995.
7. Komura, J., and Riggs, A. D. (1998) *Nucleic Acids Res. 26*, 1807−1811.
8. Xu, J., Wu, J., and Dedon, P. C. (1998) *Biochemistry 37*, 1890−1897.
9. Temple, M. D., Cairns, M. J., Denny, W. A., and Murray, V. (1997) *Nucleic Acids Res. 25*, 3255−3260.
10. Rodriguez, H., Drouin, R., Holmquist, G. P., O'Connor, T. R., Boiteux, S., Laval, J., Doroshow, J. H., and Akman, S. A. (1995) *J. Biol. Chem. 270*, 17633−17640.
11. Wei, D., Maher, V. M., and McCormick, J. J. (1995) *Proc. Natl. Acad. Sci. U.S.A. 92*, 2204−2208.
12. Denissenko, M. F., Koudriakova, T. B., Smith, L., O'Connor, T. R., Riggs, A. D., and Pfeifer, G. P. (1998) *Oncogene 17*, 3007−3014.
13. Cimino, G. D., Gamper, H. B., Isaacs, S. T., and Hearst, J. E. (1985) *Annu. Rev. Biochem. 54*, 1151−1193.
14. Ussery, D. W., Hoepfner, R. W., and Sinden, R. R. (1992) *Methods Enzymol. 212*, 242−262.
15. Sinden, R. R., and Ussery, D. W. (1992) *Methods Enzymol. 212*, 319−335.
16. Kramer, P. R., Bat, O., and Sinden, R. R. (1999) *Methods Enzymol. 304*, 639−650.
17. Hanson, C. V., Shen, C. J., and Hearst, J. E. (1976) *Science 193*, 62−64.
18. Cech, T., and Pardue, M. L. (1977) *Cell 11*, 631−640.
19. Oh, D. H., and Hanawalt, P. C. (1999) *Nucleic Acids Res. 27*, 4734−4742.
20. Conconi, A., Widmer, R. M., Koller, T., and Sogo, J. M. (1989) *Cell 57*, 753−761.
21. Vos, J.-M. H., and Hanawalt, P. C. (1987) *Cell 50*, 789−799.
22. Wellinger, R. E., and Sogo, J. M. (1998) *Nucleic Acids Res. 26*, 1544−1545.
23. Matsuo, M., Kaji, K., Utakoji, T., and Hosoda, K. (1982) *J. Gerontol. 37*, 33−37.
24. Komura, J., Sheardown, S. A., Brockdorff, N., Singer-Sam, J., and Riggs, A. D. (1997) *J. Biol. Chem. 272*, 10975−10980.
25. Le Cam, L., Polanowska, J., Fajas, L., Fabbrizio, E., and Sardet, C. (1999) *BioTechniques 26*, 840−843.
26. Quivy, J.-P., and Becker, P. B. (1997) *Methods 11*, 171−179.
27. Maxam, A. M., and Gilbert, W. (1980) *Methods Enzymol. 65*, 499−560.
28. Shi, Y., Spielmann, H. P., and Hearst, J. E. (1988) *Biochemistry 27*, 5174−5178.
29. Yeung, A. T., Dinehart, W. J., and Jones, B. K. (1988) *Biochemistry 27*, 6332−6338.
30. Kanne, D., Straub, K., Rapoport, H., and Hearst, J. E. (1982) *Biochemistry 21*, 861−871.
31. Kanne, D., Rapoport, H., and Hearst, J. E. (1984) *J. Med. Chem. 27*, 531−534.
32. Hattori, K., Angel, P., Le Beau, M. M., and Karin, M. (1988) *Proc. Natl. Acad. Sci. U.S.A. 85*, 9148−9152.
33. Esposito, F., Brankamp, R. G., and Sinden, R. R. (1988) *J. Biol. Chem. 263*, 11466−11472.
34. Bordin, F., Dall'acqua, F., and Guiotto, A. (1991) *Pharmacol. Ther. 52*, 331−363.
35. Boyer, V., Moustacchi, E., and Sage, E. (1988) *Biochemistry 27*, 3011−3018.
36. Teebor, G. W., and Brent, T. P. (1981) in *DNA Repair: A Laboratory Manual of Research Procedures* (Friedberg, E. C., and Hanawalt, P. C., Eds.) Vol. 1, part A, pp 203−212, Marcel Dekker, New York.
37. Friedberg, E. C., Walker, G. C., and Siede, W. (1995) *DNA Repair and Mutagenesis*, ASM Press, Washington, DC.
38. Rozek, D., and Pfeifer, G. P. (1993) *Mol. Cell. Biol. 13*, 5490−5499.
39. Rozek, D., and Pfeifer, G. P. (1995) *J. Cell. Biochem. 57*, 479−487.
40. Tornaletti, S., and Pfeifer, G. P. (1995) *J. Mol. Biol. 249*, 714−728.
41. Janknecht, R., Cahill, M. A., and Nordheim, A. (1995) *Carcinogenesis 16*, 443−450.
42. Herrera, R. E., Nordheim, A., and Stewart, A. F. (1997) *Chromosoma 106*, 284−292.
43. Herrera, R. E., Shaw, P. E., and Nordheim, A. (1989) *Nature 340*, 68−70.
44. Runkel, L., Shaw, P. E., Herrera, R. E., Hipskind, R. A., and Nordheim, A. (1991) *Mol. Cell. Biol. 11*, 1270−1280.
45. Dey, A., Nebert, D. W., and Ozato, K. (1991) *DNA Cell Biol. 10*, 537−544.
46. Konig, H. (1991) *Nucleic Acids Res. 19*, 3607−3611.
47. Schild-Poulter, C., Sassone-Corsi, P., Granger-Schnarr, M., and Schnarr, M. (1996) *Nucleic Acids Res. 24*, 4751−4758.
48. Sogo, J. M., Stahl, H., Koller, T., and Knippers, R. (1986) *J. Mol. Biol. 189*, 189−204.
49. Zhen, W., Jeppesen, C., and Nielsen, P. E. (1988) *FEBS Lett. 229*, 73−76.
50. Potter, D. A., Fostel, J. M., Berninger, M., Pardue, M. L., and Cech, T. R. (1980) *Proc. Natl. Acad. Sci. U.S.A. 77*, 4118−4122.
51. Sinden, R. R., Carlson, J. O., and Pettijohn, D. E. (1980) *Cell 21*, 773−783.
52. Kochel, T. J., and Sinden, R. R. (1989) *J. Mol. Biol. 205*, 91−102.
53. Chen, T. A., and Allfrey, V. G. (1987) *Proc. Natl. Acad. Sci. U.S.A. 84*, 5252−5256.
54. Murphy, D. J., Hardy, S., and Engel, D. A. (1999) *Mol. Cell. Biol. 19*, 2724−2733.
55. Van Houten, B., Gamper, H., Hearst, J. E., and Sancar, A. (1986) *J. Biol. Chem. 261*, 14135−14141.
56. Thomas, D. C., Morton, A. G., Bohr, V. A., and Sancar, A. (1988) *Proc. Natl. Acad. Sci. U.S.A. 85*, 3723−3727.

BI002539F